

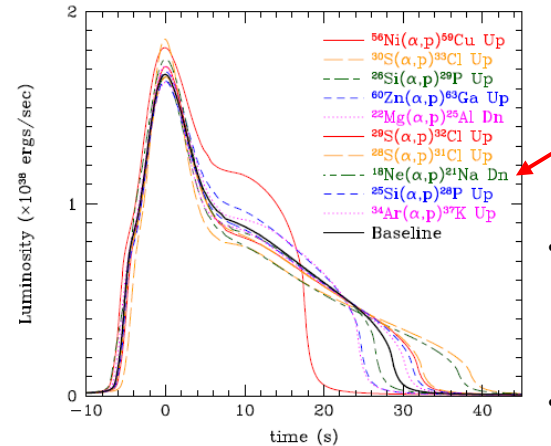
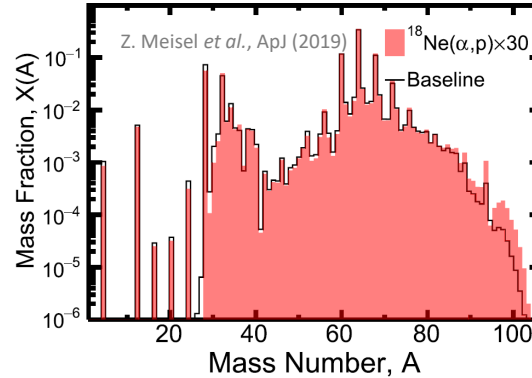
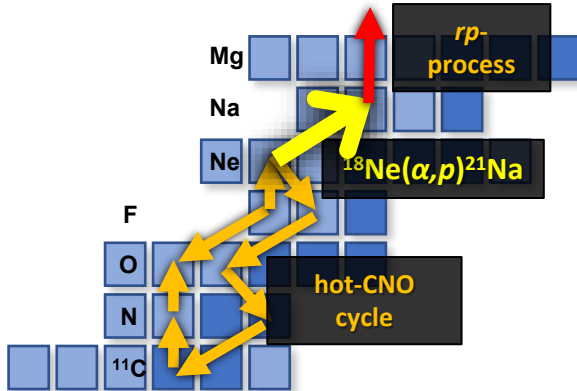
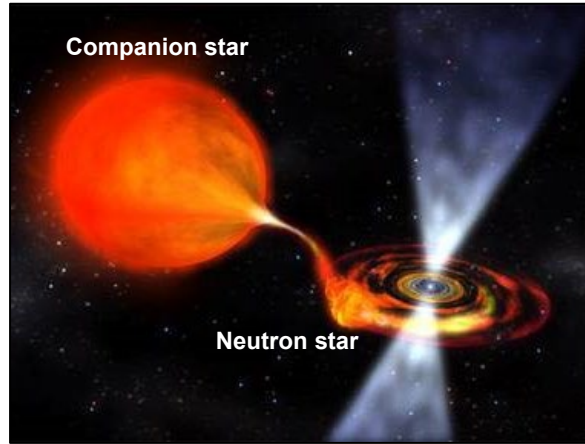
Experimental study on astrophysically important ^{22}Mg nucleus via resonant scattering of $^{18}\text{Ne} + \alpha$

Soomi Cha

**Center for Exotic Nuclear Studies,
Institute for Basic Science**

Background Image:
Courtesy of J. DePasquale.

$^{18}\text{Ne}(\alpha, p)^{21}\text{Na}$ reaction



Rank	Reaction	Type ^a	Sensitivity ^b	Category
1	$^{15}\text{O}(\alpha, \gamma)^{19}\text{Ne}$	D	16	1
2	$^{56}\text{Ni}(\alpha, p)^{59}\text{Cu}$	U	6.4	1
3	$^{59}\text{Cu}(p, \gamma)^{60}\text{Zn}$	D	5.1	1
4	$^{61}\text{Ga}(p, \gamma)^{62}\text{Ge}$	D	3.7	1
5	$^{22}\text{Mg}(\alpha, p)^{25}\text{Al}$	D	2.3	1
6	$^{14}\text{O}(\alpha, p)^{17}\text{F}$	D	5.8	1
7	$^{23}\text{Al}(p, \gamma)^{24}\text{Si}$	D	4.6	1
8	$^{18}\text{Ne}(\alpha, p)^{21}\text{Na}$	U	1.8	1
9	$^{63}\text{Ga}(p, \gamma)^{64}\text{Ge}$	D	1.4	2
10	$^{19}\text{F}(p, \alpha)^{16}\text{O}$	U	1.3	2
11	$^{12}\text{C}(\alpha, \gamma)^{16}\text{O}$	U	2.1	2
12	$^{26}\text{Si}(\alpha, p)^{29}\text{P}$	U	1.8	2
13	$^{17}\text{F}(\alpha, p)^{20}\text{Ne}$	U	3.5	2
14	$^{24}\text{Mg}(\alpha, \gamma)^{28}\text{Si}$	U	1.2	2
15	$^{57}\text{Cu}(p, \gamma)^{58}\text{Zn}$	D	1.3	2
16	$^{60}\text{Zn}(\alpha, p)^{63}\text{Ga}$	U	1.1	2
17	$^{17}\text{F}(p, \gamma)^{18}\text{Ne}$	U	1.7	2
18	$^{40}\text{Sc}(p, \gamma)^{41}\text{Ti}$	D	1.1	2
19	$^{48}\text{Cr}(p, \gamma)^{49}\text{Mn}$	D	1.2	2

R. H. Cyburt *et al.*, ApJ (2016)

- one of the break-out candidates from the hot-CNO cycle, fueling the *rp*-process

R. Wallace & S. Woosely, ApJ. S. (1981)

- affects on the characteristics of X-ray burst (light curve, ash composition)

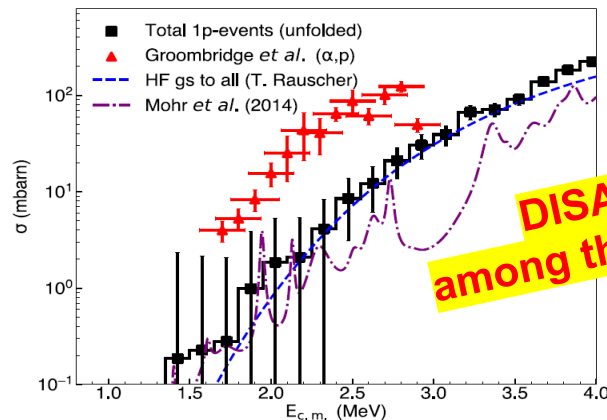
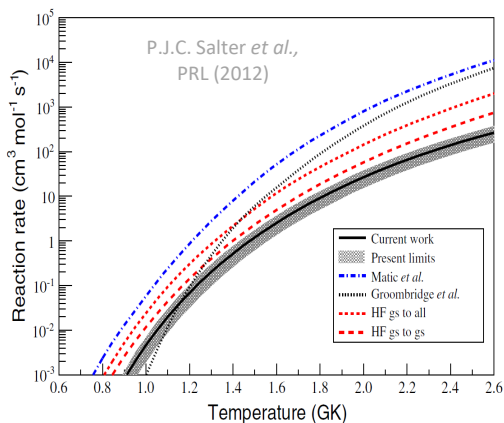
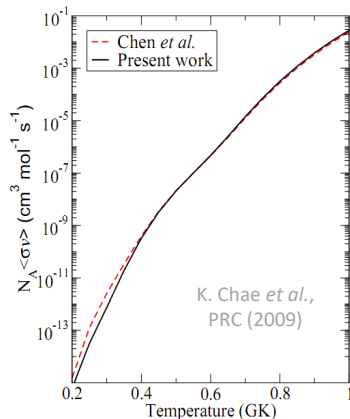
Previous studies on the $^{18}\text{Ne}(\alpha,p)^{21}\text{Na}$ reaction

Indirect measurements

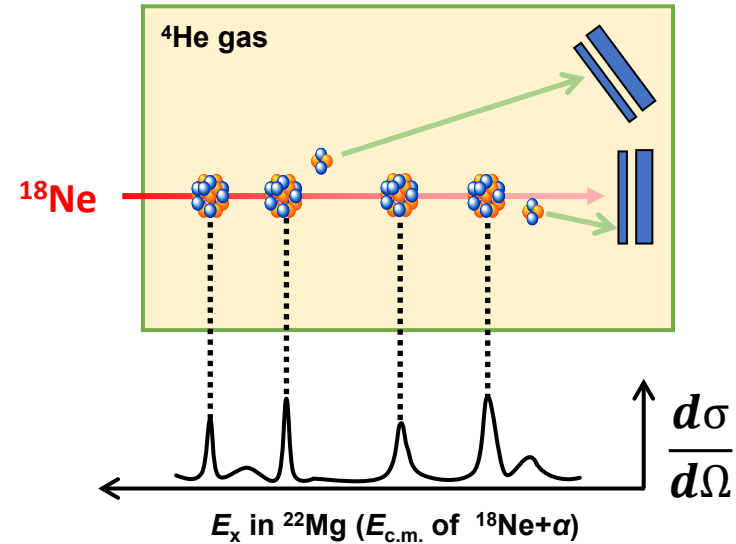
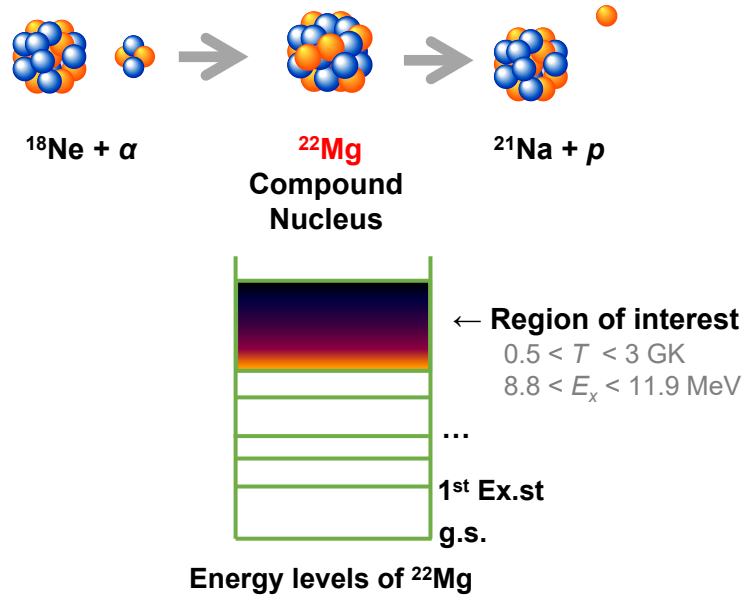
- **studies of the structure of ^{22}Mg**
 - $^{24}\text{Mg}(p,t)^{22}\text{Mg}$, $^{12}\text{C}(^{16}\text{O},^6\text{He})^{22}\text{Mg}$, $^{25}\text{Mg}(^3\text{He},^6\text{He})^{22}\text{Mg}$, ...
 - several resonance parameters obtained
- **time reversal reaction : $^{21}\text{Na}(p,a)^{18}\text{Ne}$**
 - Salter *et al.*, PRL(2012) : $E_{\text{cm}} = 1.19\text{-}2.57$ MeV
 - only (a,p_0) measured \rightarrow considered as a lower limit

Direct measurements

- **two measurements at Louvain-la-Neuve**
 - Bradfield-Smith *et al.*, PRC (1999) : $E_{\text{cm}} = 2.0\text{-}3.0$ MeV
 - Groombridge *et al.*, PRC (2002) : $E_{\text{cm}} = 1.7\text{-}2.9$ MeV
- **recent measurement at FSU**
 - Anastasiou *et al.*, PRC (2022) : $E_{\text{cm}} = 2.5\text{-}4$ MeV



M. Anastasiou *et al.*, PRC (2022)



- Energy level properties of ^{22}Mg above the $E_{\alpha\text{-thres.}}$ dominates the $^{18}\text{Ne}(\alpha, p)^{21}\text{Na}$ reaction
- $^{18}\text{Ne} + \alpha$ resonant scattering can populate the energy levels of ^{22}Mg !
- Thick target method in inverse kinematics adopted.

K. P. Artemov *et al.*, Sov. J. Nucl. Phys. 52, 408 (1990)

Theoretical Prediction

M. Dufour & P. Descouvemont, NPA (2003)

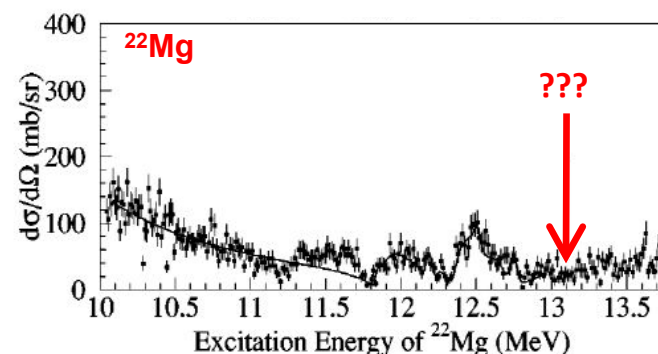
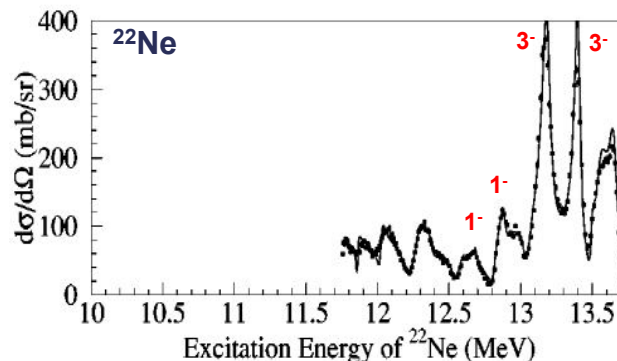
ETCM calculation : ^{22}Ne		
J^π	E_x (MeV)	θ_α^2 (%)
1^-	12.58	13
1^-	13.53	8
3^-	12.92	13
3^-	13.69	11

GCM calculation : ^{22}Mg		
J^π	E_x (MeV)	θ_α^2 (%)
1^-	12.14	11.5
1^-	13.04	6.7
3^-	12.46	11.6
3^-	13.19	11.7

Experiment

G.V. Rogachev *et al.*, PRC (2001)

V. Goldberg *et al.*, PRC (2004)



- Predicted 1^- and 3^- doublets arose from the α -cluster structure in ^{22}Mg
- Not observed in the previous experiment

$^{18}\text{Ne} + \alpha$ resonant scattering

ETCM calculation : ^{22}Ne

E_x (MeV)	θ_{α}^2 (%)
12.58	13

GCM calculation : ^{22}Mg

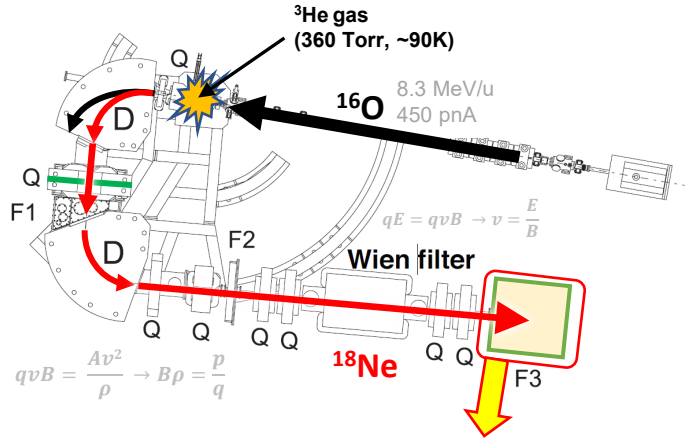
J^{π}	E_x (MeV)	θ_{α}^2 (%)
1^{-}	12.14	11.5

1. To enhance our knowledges on the $^{18}\text{Ne}(\alpha, p)^{21}\text{Na}$ reaction
2. Observation of 1^{-} and 3^{-} states could be the evidence of the α -cluster states in ^{22}Mg nucleus.
3. Investigating wide energy range will provide the first spectroscopic study for $E_x > 14$ MeV !

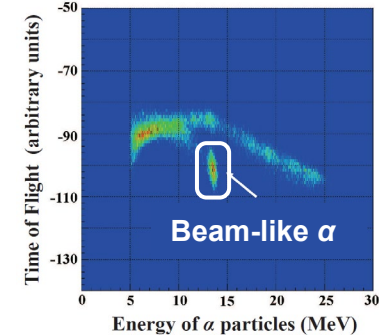
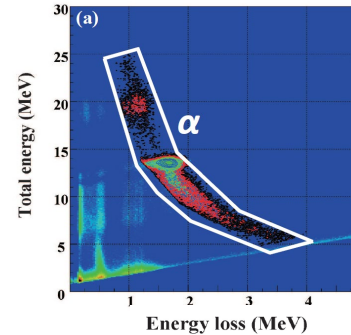
- Predicted 1^{-} and 3^{-} doublets arose from the α -cluster structure in ^{22}Mg
- Not observed in the previous experiment

$^{18}\text{Ne}(\alpha,\alpha)^{18}\text{Ne}$ measurement at CRIB

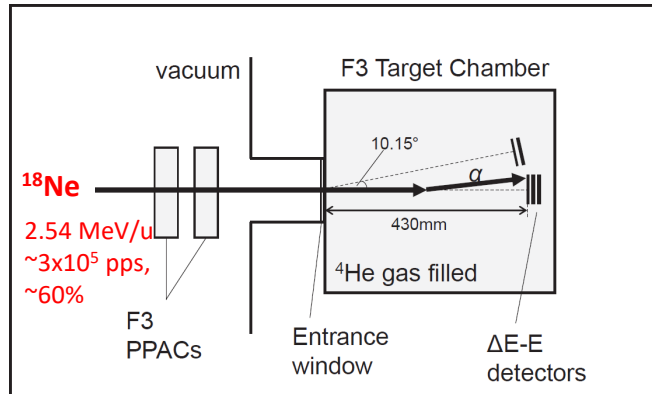
CNS Radio-Isotope Beam separator



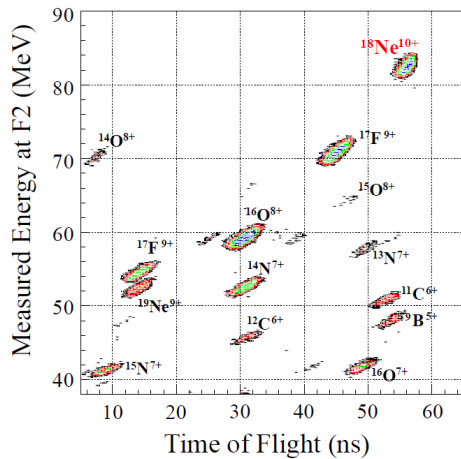
- ^{18}Ne beam produced by In-flight fragment : $^{16}\text{O}(^3\text{He},n)^{18}\text{Ne}$
- recoiling α particle measurement by silicon detector telescopes (energy, position)



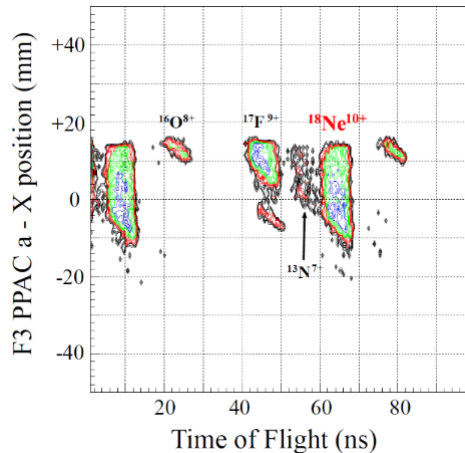
- Tracks of ^{18}Ne beam particles obtained by two PPACs (extrapolation)
- kinematics reconstruction by considering the energy loss of the beam and recoiling α particles
- Excitation function of ^{22}Mg extracted !**



$^{18}\text{Ne}(\alpha,\alpha)^{18}\text{Ne}$ measurement at CRIB



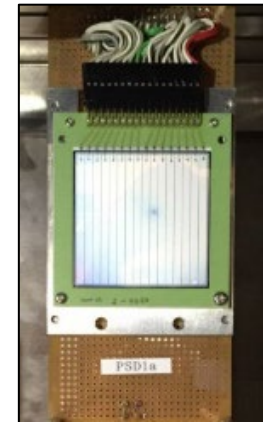
F2 : RI beam ID



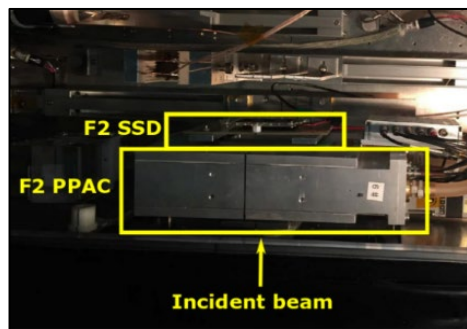
F3 : purified ^{18}Ne beam !



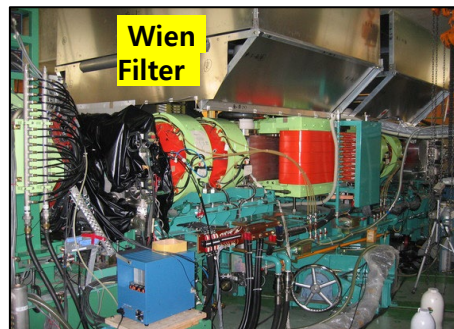
Silicon detector telescopes for energy and position measurement



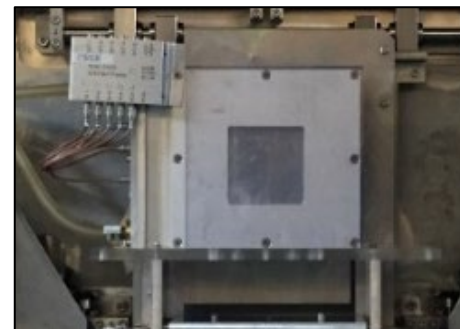
Beam monitoring /Beam trajectory extrapolation by two F3 PPACs



A bird eye's view of F2 focal plane

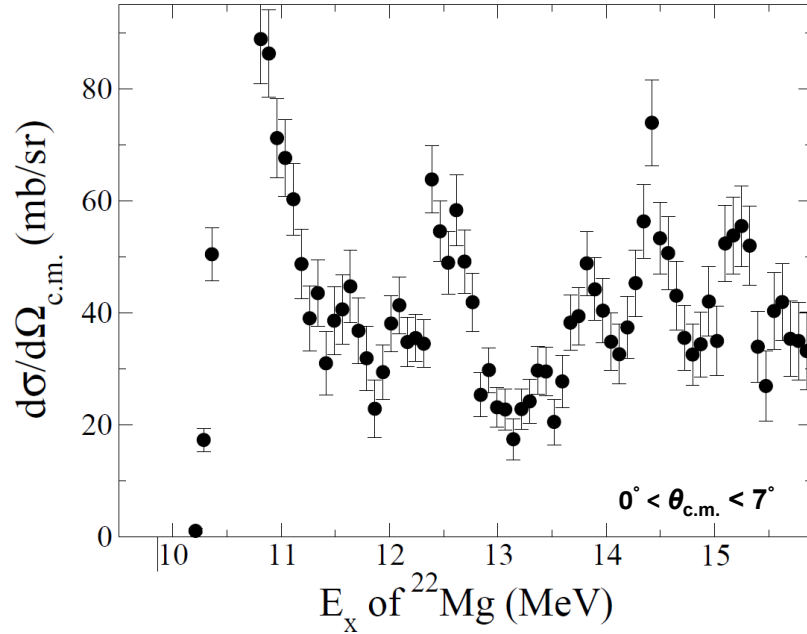


CRIB Wien Filter



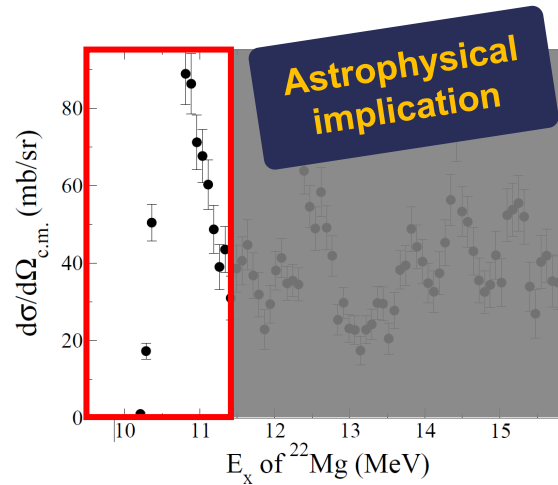
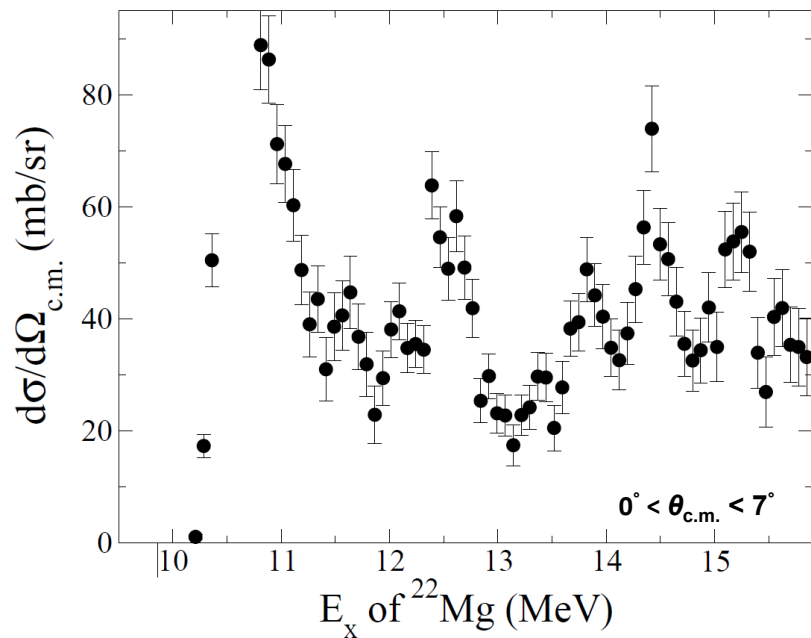
Excitation function of $^{18}\text{Ne}+\alpha$ system (^{22}Mg)

$$\left(\frac{d\sigma}{d\Omega}\right)_{\text{c.m.}} = \frac{1}{4 \cos \theta_{\text{lab}}} \left(\frac{d\sigma}{d\Omega}\right)_{\text{lab}} = \frac{1}{4 \cos \theta_{\text{lab}}} \frac{Y}{IN\Delta\Omega_{\text{lab}}}$$



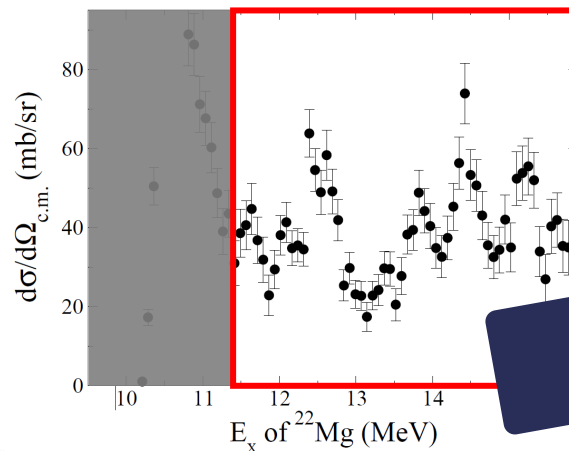
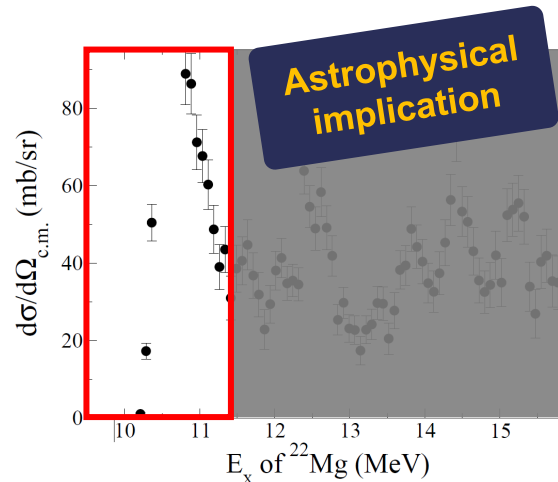
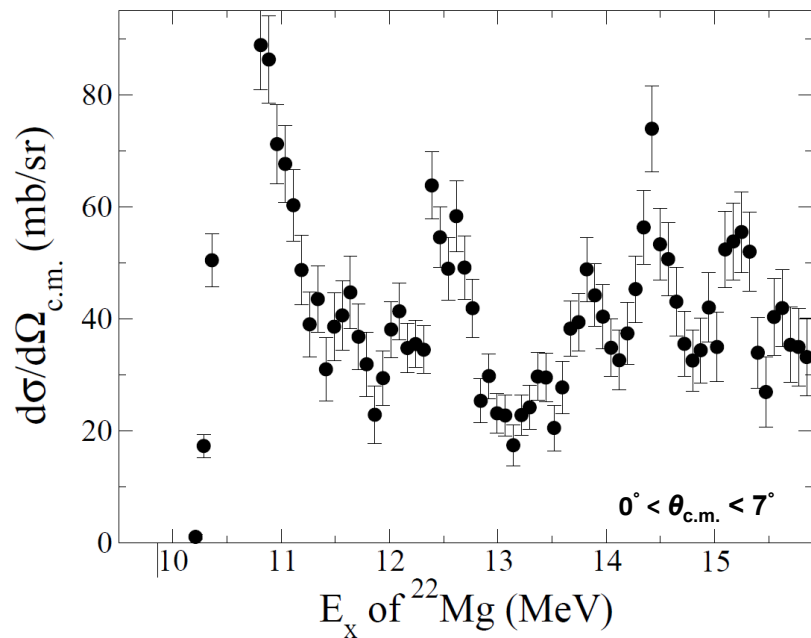
Excitation function of $^{18}\text{Ne}+\alpha$ system (^{22}Mg)

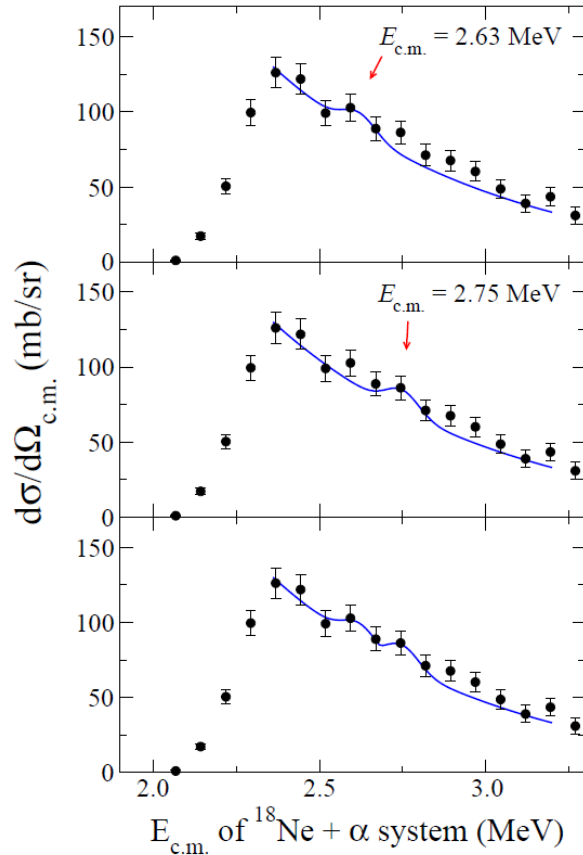
$$\left(\frac{d\sigma}{d\Omega}\right)_{\text{c.m.}} = \frac{1}{4 \cos \theta_{\text{lab}}} \left(\frac{d\sigma}{d\Omega}\right)_{\text{lab}} = \frac{1}{4 \cos \theta_{\text{lab}}} \frac{Y}{IN\Delta\Omega_{\text{lab}}}$$



Excitation function of $^{18}\text{Ne}+\alpha$ system (^{22}Mg)

$$\left(\frac{d\sigma}{d\Omega}\right)_{\text{c.m.}} = \frac{1}{4 \cos \theta_{\text{lab}}} \left(\frac{d\sigma}{d\Omega}\right)_{\text{lab}} = \frac{1}{4 \cos \theta_{\text{lab}}} \frac{Y}{IN\Delta\Omega_{\text{lab}}}$$



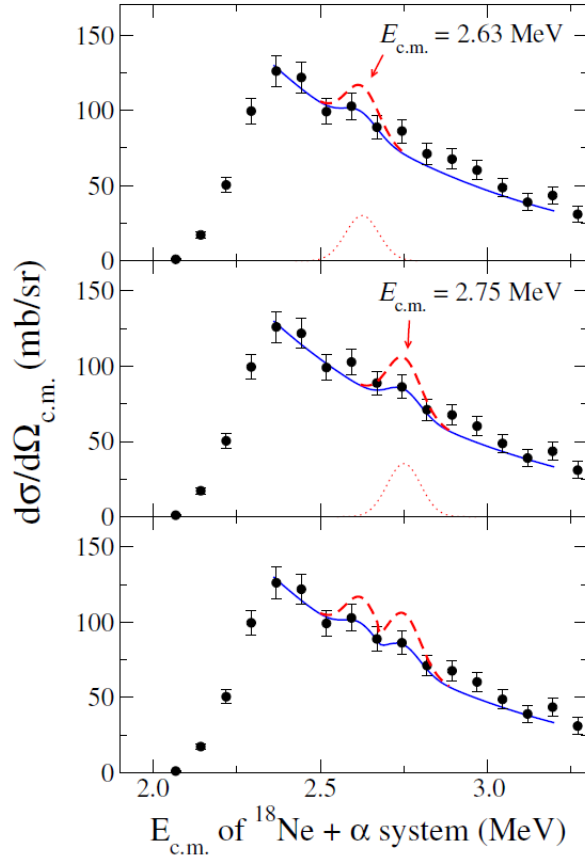


- **Two small bumps were observed** at the astrophysically important energy range ($T_9 < 2$ GK $\leftrightarrow E_x < 2.9$ MeV)
- Two energy levels have been reported in the previous direct measurement.

Present Work	Groombridge <i>et al.</i>
$E_{c.m.}$ (MeV)	$E_{c.m.}$ (MeV)
2.63	2.52 ± 0.14
2.75	2.72 ± 0.14

$dE_{cm}=50\text{-}100\text{keV}$

- The existence of these resonances is not obvious in our data possibly due to the insufficient statistics.

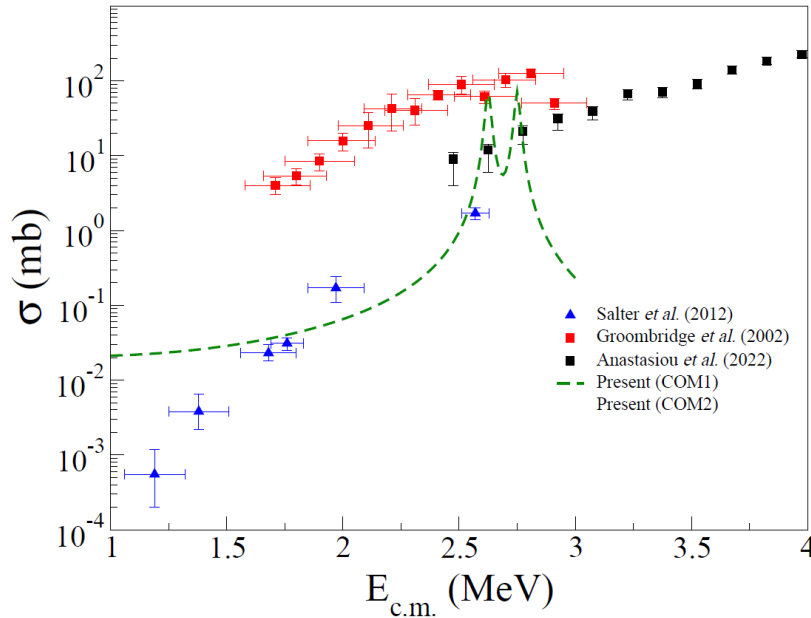


- **Two small bumps were observed** at the astrophysically important energy range ($T_9 < 2$ GK $\leftrightarrow E_x < 2.9$ MeV)
- Two energy levels have been reported in the previous direct measurement.

Present Work	Groombridge et al.
$E_{c.m.}$ (MeV)	$E_{c.m.}$ (MeV)
2.63	2.52 ± 0.14
2.75	2.72 ± 0.14

$dE_{cm}=50\text{-}100\text{keV}$

- The existence of these resonances is not obvious in our data possibly due to the insufficient statistics.
- **Upper limits on the $^{18}\text{Ne}(\alpha,\alpha)^{18}\text{Ne}$ cross section were set (one-sigma confidence level).**



- $^{18}\text{Ne}(\alpha,p)^{21}\text{Na}$ reaction cross section was calculated using the Breit-Wigner formula.

$$\sigma_{BW}(E) = \frac{\lambda^2}{4\pi} \frac{(2J_r + 1)}{(2J_{\text{Ne}} + 1)(2J_{\alpha} + 1)} \frac{\Gamma_{\alpha}\Gamma_p}{(E - E_r)^2 + (\Gamma_{\text{tot}}/2)^2}$$

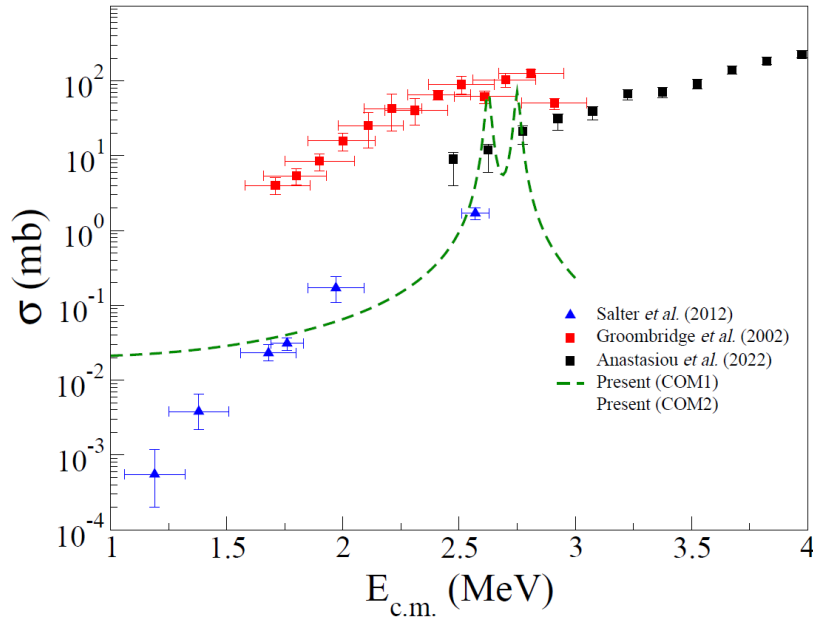
- E_r, Γ_{α} adopted from the two observed bumps
- J^{π} adopted as 0^{+}

D. Groombridge *et al.*, PRC (2002)

- Γ_p in this energy region has not been reported
→ approximated Γ_p by two different approaches!

considering the Wigner limit, global mean reduced proton width, ...
assuming $\Gamma_{\text{tot}} = \Gamma_{\alpha} + \Gamma_p$ & Γ_{tot} adopted from Groombridge *et al.*

	E_r	J^{π}	Γ_{α}	Γ_p	Γ_{tot}
COM1	2.63	0^{+}	0.015	0.01	0.025
	2.75	0^{+}	0.015	0.01	0.025
COM2	2.63	0^{+}	0.015	0.085	0.1
	2.75	0^{+}	0.015	0.195	0.21



- $^{18}\text{Ne}(\alpha,p)^{21}\text{Na}$ reaction cross section was calculated using the Breit-Wigner formula.

$$\sigma_{BW}(E) = \frac{\lambda^2}{4\pi} \frac{(2J_r + 1)}{(2J_{\text{Ne}} + 1)(2J_{\alpha} + 1)} \frac{\Gamma_{\alpha}\Gamma_p}{(E - E_r)^2 + (\Gamma_{\text{tot}}/2)^2}$$

- E_r, Γ_{α} adopted from the two observed bumps

- J^{π} adopted as 0^{+}

D. Groombridge *et al.*, PRC (2002)

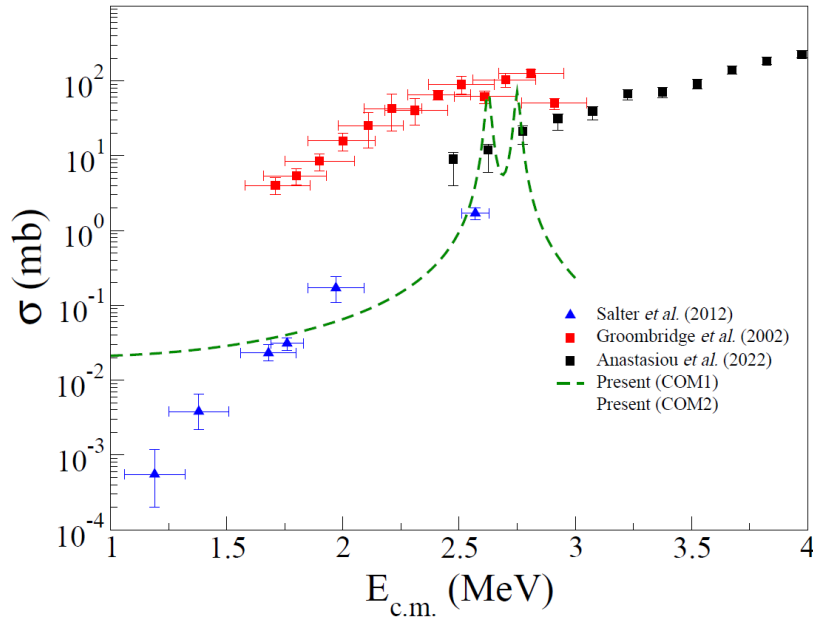
- Γ_p in this energy region has not been reported

→ approximated Γ_p by two different approaches!

considering the Wigner limit, global mean reduced proton width, ...

assuming $\Gamma_{\text{tot}} = \Gamma_{\alpha} + \Gamma_p$ & Γ_{tot} adopted from Groombridge *et al.*

	E_r	J^{π}	Γ_{α}	Γ_p	Γ_{tot}
COM1	2.63	0^{+}	0.015	0.01	0.025
	2.75	0^{+}	0.015	0.01	0.025
COM2	2.63	0^{+}	0.015	0.085	0.1
	2.75	0^{+}	0.015	0.195	0.21



- $^{18}\text{Ne}(\alpha,p)^{21}\text{Na}$ reaction cross section was calculated using the Breit-Wigner formula.

$$\sigma_{BW}(E) = \frac{\lambda^2}{4\pi} \frac{(2J_r + 1)}{(2J_{\text{Ne}} + 1)(2J_{\alpha} + 1)} \frac{\Gamma_{\alpha}\Gamma_p}{(E - E_r)^2 + (\Gamma_{\text{tot}}/2)^2}$$

- E_r, Γ_{α} adopted from the two observed bumps

- J^{π} adopted as 0^{+}

D. Groombridge *et al.*, PRC (2002)

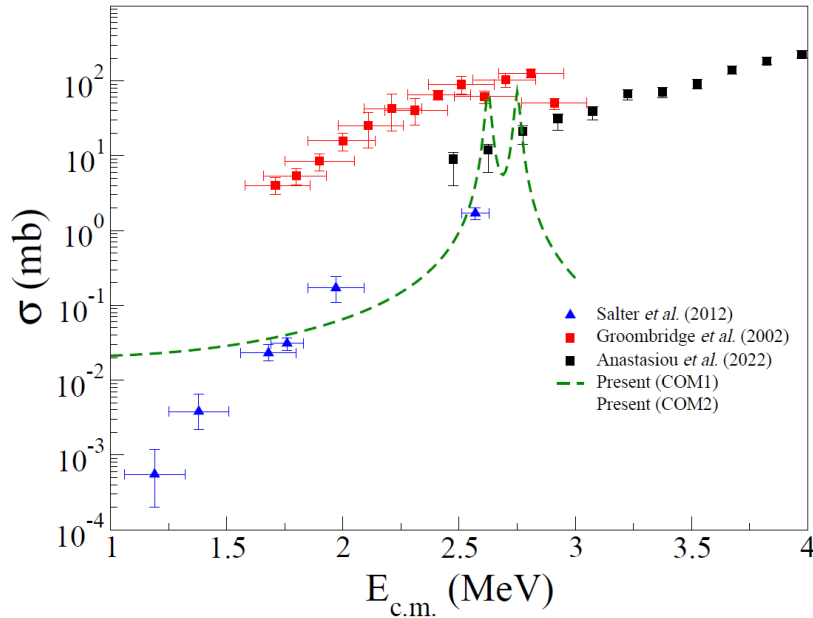
- Γ_p in this energy region has not been reported

→ approximated Γ_p by two different approaches!

considering the Wigner limit, global mean reduced proton width, ...

assuming $\Gamma_{\text{tot}} = \Gamma_{\alpha} + \Gamma_p$ & Γ_{tot} adopted from Groombridge *et al.*

	E_r	J^{π}	Γ_{α}	Γ_p	Γ_{tot}
COM1	2.63	0^{+}	0.015	0.01	0.025
	2.75	0^{+}	0.015	0.01	0.025
COM2	2.63	0^{+}	0.015	0.085	0.1
	2.75	0^{+}	0.015	0.195	0.21



- $^{18}\text{Ne}(\alpha,p)^{21}\text{Na}$ reaction cross section was calculated using the Breit-Wigner formula.

$$\sigma_{BW}(E) = \frac{\lambda^2}{4\pi} \frac{(2J_r + 1)}{(2J_{\text{Ne}} + 1)(2J_{\alpha} + 1)} \frac{\Gamma_{\alpha} \Gamma_p}{(E - E_r)^2 + (\Gamma_{\text{tot}}/2)^2}$$

- E_r , Γ_{α} adopted from the two observed bumps

- J^{π} adopted as 0^{+}

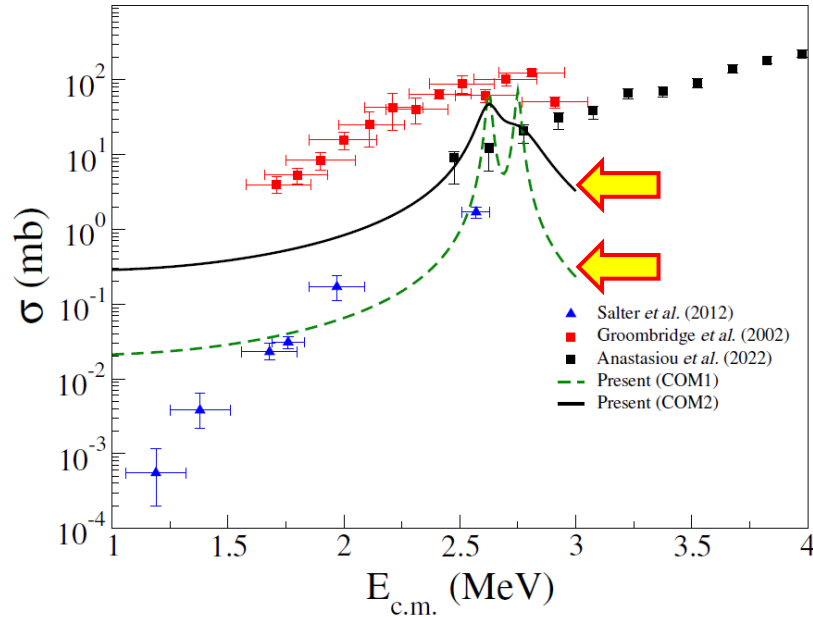
D. Groombridge *et al.*, PRC (2002)

- Γ_p in this energy region has not been reported

→ **approximated Γ_p by two different approaches!**

considering the Wigner limit, global mean reduced proton width, ...
assuming $\Gamma_{\text{tot}} = \Gamma_{\alpha} + \Gamma_p$ & Γ_{tot} adopted from Groombridge *et al.*

	E_r	J^{π}	Γ_{α}	Γ_p	Γ_{tot}
COM1	2.63	0^{+}	0.015	0.01	0.025
	2.75	0^{+}	0.015	0.01	0.025
COM2	2.63	0^{+}	0.015	0.085	0.1
	2.75	0^{+}	0.015	0.195	0.21



- $^{18}\text{Ne}(\alpha,p)^{21}\text{Na}$ reaction cross section was calculated using the Breit-Wigner formula.

$$\sigma_{BW}(E) = \frac{\lambda^2}{4\pi} \frac{(2J_r + 1)}{(2J_{\text{Ne}} + 1)(2J_{\alpha} + 1)} \frac{\Gamma_{\alpha} \Gamma_p}{(E - E_r)^2 + (\Gamma_{\text{tot}}/2)^2}$$

- E_r , Γ_{α} adopted from the two observed bumps
- J^{π} adopted as 0^{+}

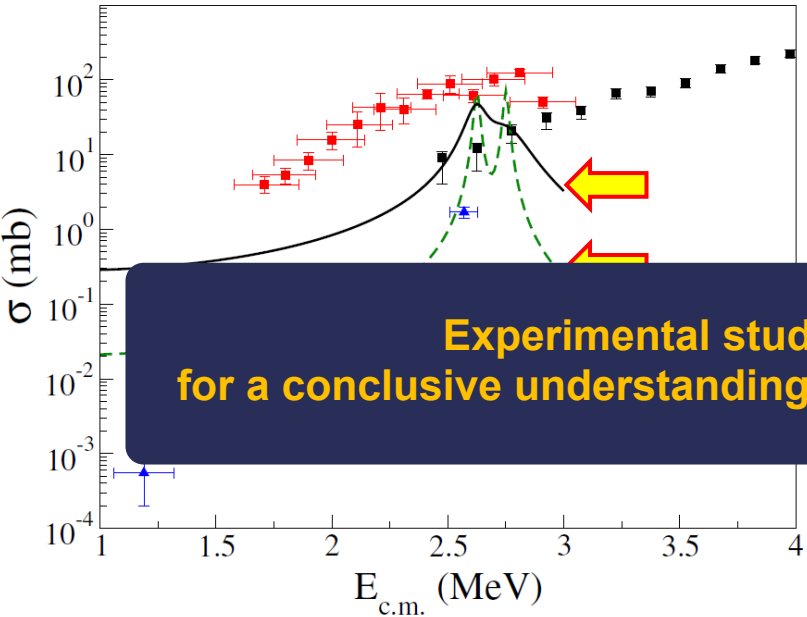
D. Groombridge *et al.*, PRC (2002)

- Γ_p in this energy region has not been reported
→ approximated Γ_p by two different approaches!

considering the Wigner limit, global mean reduced proton width, ...
assuming $\Gamma_{\text{tot}} = \Gamma_{\alpha} + \Gamma_p$ & Γ_{tot} adopted from Groombridge *et al.*

	E_r	J^{π}	Γ_{α}	Γ_p	Γ_{tot}
COM1	2.63	0^{+}	0.015	0.01	0.025
	2.75	0^{+}	0.015	0.01	0.025
COM2	2.63	0^{+}	0.015	0.085	0.1
	2.75	0^{+}	0.015	0.195	0.21

$^{18}\text{Ne}(\alpha,p)^{21}\text{Na}$ reaction cross section strongly depend on the proton widths of the resonances!



- $^{18}\text{Ne}(\alpha,p)^{21}\text{Na}$ reaction cross section was calculated using the Breit-Wigner formula.

$$\sigma_{BW}(E) = \frac{\lambda^2}{4\pi} \frac{(2J_r + 1)}{(2J_{\text{Ne}} + 1)(2J_{\alpha} + 1)} \frac{\Gamma_{\alpha}\Gamma_p}{(E - E_r)^2 + (\Gamma_{\text{tot}}/2)^2}$$

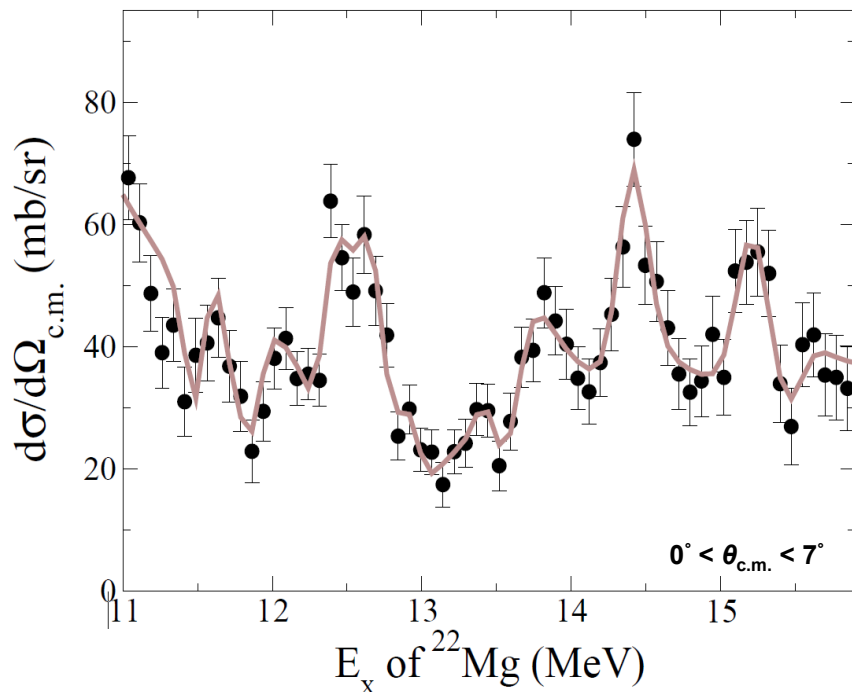
Experimental studies of the Γ_p are highly required for a conclusive understanding on the $^{18}\text{Ne}(\alpha,p)^{21}\text{Na}$ reaction cross section !

S.M. Cha et al., Frontiers in Physics (2023)
→ approximated by different approaches!

considering the Wigner limit, global mean reduced proton width, ...
assuming $\Gamma_{\text{tot}} = \Gamma_{\alpha} + \Gamma_p$ & Γ_{tot} adopted from Groombridge *et al.*

	E_r	J^{π}	Γ_{α}	Γ_p	Γ_{tot}
COM1	2.63	0^{+}	0.015	0.01	0.025
	2.75	0^{+}	0.015	0.01	0.025
COM2	2.63	0^{+}	0.015	0.085	0.1
	2.75	0^{+}	0.015	0.195	0.21

$^{18}\text{Ne}(\alpha,p)^{21}\text{Na}$ reaction cross section strongly depend on the proton widths of the resonances !



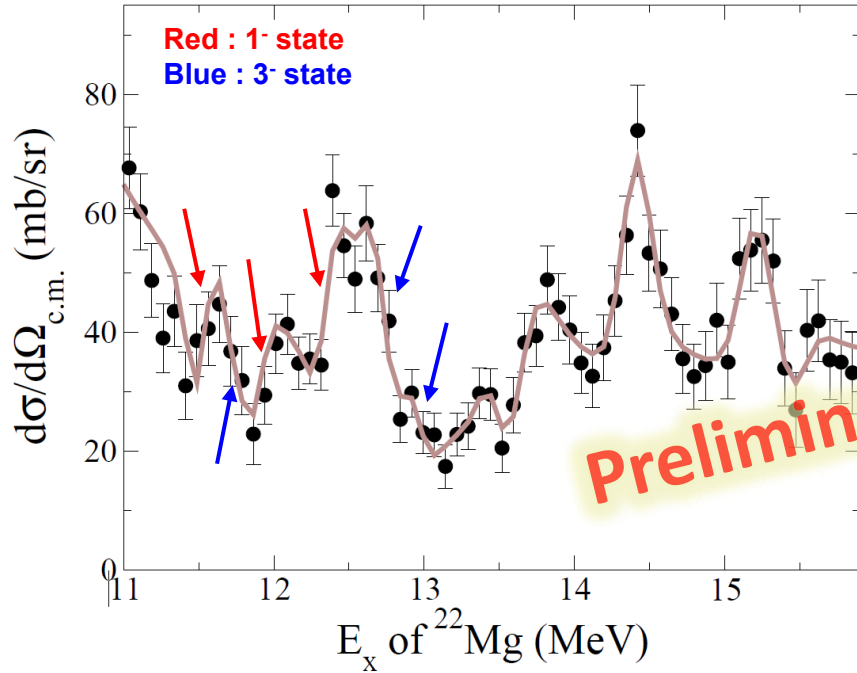
- **Evident peaks** observed at $E_x \sim 11 - 16$ MeV !
- Resonance parameters of ^{22}Mg nucleus ($E_r, \Gamma_\alpha, J^\pi$) can be constrained by **R-matrix analysis**.
- performed R-matrix calculation using SAMMY8
- All possible spin and natural parity combinations was considered during the analysis.
- χ^2 analysis is performed to deduce possible resonance parameters for each peak.

- calculated the dimensionless partial width (θ_α^2) for each level to provide a direct comparison with theoretical prediction

$$\theta_\alpha^2 = \Gamma_\alpha / \Gamma_W$$

$$\Gamma_w = 2\hbar^2 / \mu R^2 P_l$$

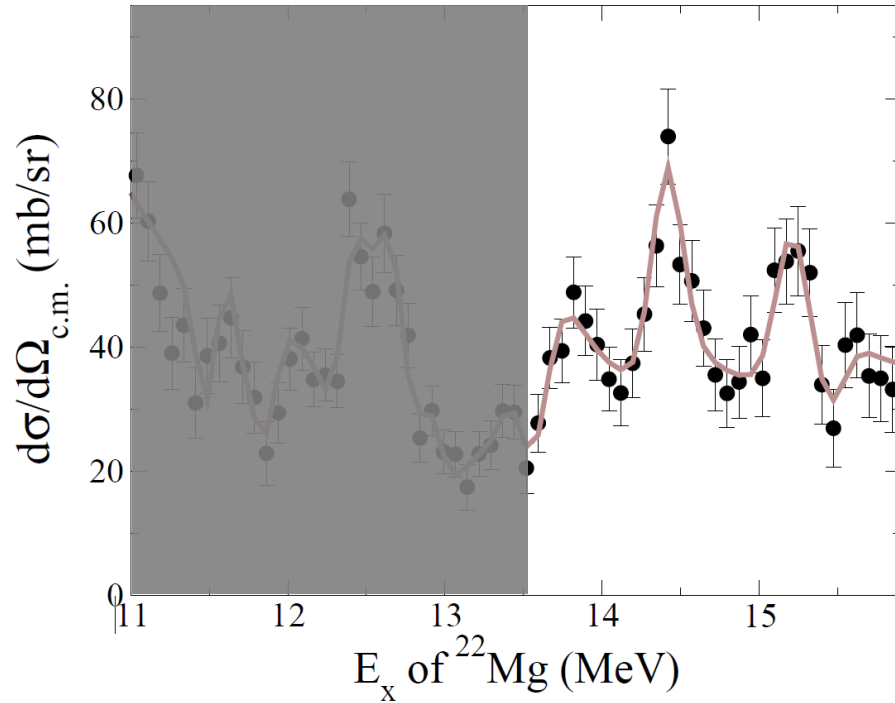
1⁻ and 3⁻ candidates ?



- Cluster model (CM) and Shell model (SM) calculation performed
- 1⁻ states obtained from both CM and SM calculation
- More discussions on 3⁻ states and reduction of α -widths required

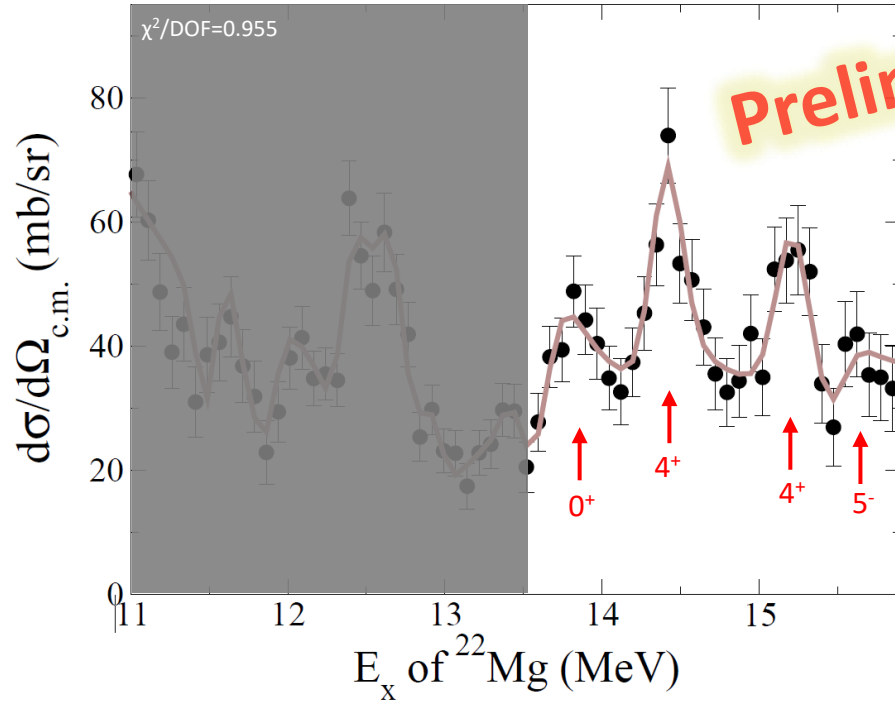
Present Work				Dufour & Descouvemont			Goldberg <i>et al.</i>	
E_x (MeV)	Γ_α (keV)	J^π	θ_α^2 (%)	E_x^{GCM} (MeV)	J^π	θ_α^{2GCM} (%)	E_x (MeV)	J
11.493	7	1 ⁻	4.78	12.25	1 ⁻	11.5	11.462	1
11.705	3	3 ⁻	12.30	12.57	3 ⁻	11.6	11.798	2
11.869	6	1 ⁻	2.40	13.15	1 ⁻	6.7	11.842	1
12.352	19	1 ⁻ (4 ⁺)	3.72	13.30	3 ⁻	11.7	11.9	0
12.744	11	3 ⁻	6.80				12.362	1
12.974	8	3 ⁻	3.65					
13.456	4	3 ⁻ (0 ⁺ , 1 ⁻)	1.06					

First spectroscopic result of ^{22}Mg



- No information from NNDC
- No information from the theory

First spectroscopic result of ^{22}Mg



Present work			
E_x (MeV)	Γ_α (keV)	J^π	θ_a^2 (%)
13.644	177	0^+ ($1^-, 4^+, 5^-$)	11.0
14.381	16	4^+ ($2^+, 5^-$)	5.01
15.199	15	4^+ ($2^+, 3^-$)	2.49
15.477	4	5^- ($0^+ \text{ to } 7^-$)	1.59

- Best fitting result : $J^\pi = 0^+, 4^+, 4^+, \text{ and } 5^-$ for four peaks
- cannot exclude other possibilities

- The α resonant scattering on ^{18}Ne was measured in inverse kinematics to understand the astrophysically important $^{18}\text{Ne}(\alpha, p)^{21}\text{Na}$ reaction and the α -clustering of proton-rich ^{22}Mg nucleus.
- The measurement of $^{18}\text{Ne} + \alpha$ scattering was done at CRIB in RIKEN by adopting the thick target method.
- The excitation function of ^{22}Mg was obtained for $E_x = 10\text{--}16$ MeV.
- Since energy levels were not clearly observed at the astrophysically important energy range, upper limits on the $^{18}\text{Ne}(\alpha, \alpha)^{18}\text{Ne}$ cross section were set.
- The astrophysical impact was also investigated by estimating the $^{18}\text{Ne}(\alpha, p)^{21}\text{Na}$ cross section.
- R-matrix analysis was performed to constrain the energy level properties of ^{22}Mg .



Background Image:
Courtesy of Tervel Kutsev
Astronomical Photographer of the year 2023
“People and Space” category

List of collaborators

CENS, IBS	S.M.Cha, S.H.Bae, K.I.Hahn, D.Kim, B.Moon
Sungkyunkwan U.	K.Y.Chae*, N.N.Duy, M.J.Kim, E.J.Lee
U. of Tokyo	K.Abe, S.Hayakawa, H.Shimizu, H.Yamaguchi, L.Yang
Seoul National U.	S.H.Choi
30 MeV Cyclotron center	D.N.Binh
RIKEN Nishina Center	V.H.Phong, Z. Ge
Ewha Womans U.	A.Kim, G.W.Kim, S.I.Lim, S.Y.Park
Korea U.	B.Hong
U. of Edinburgh	D.Kahl
Vietnam A. of Sci. and Tech.	L.H.Khiem
Chonbuk National U.	E.J.Kim
IRIS, IBS	J.Y.Moon, M.S.Kwag
UNIST	K.Kwak

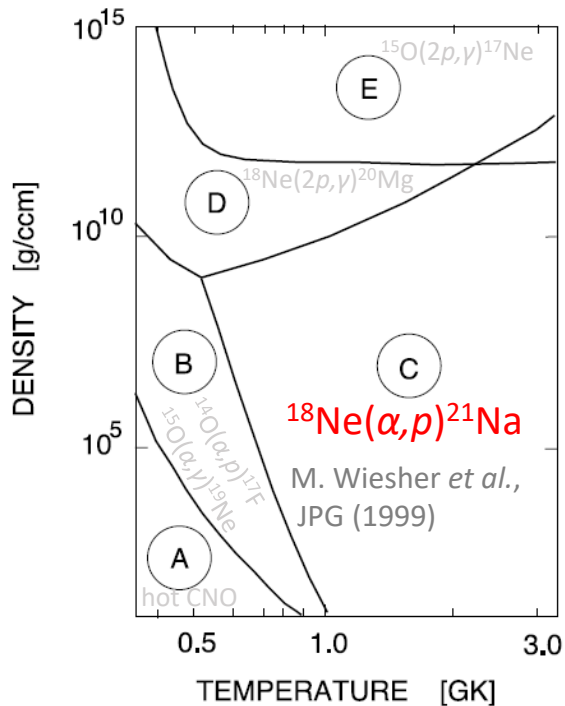
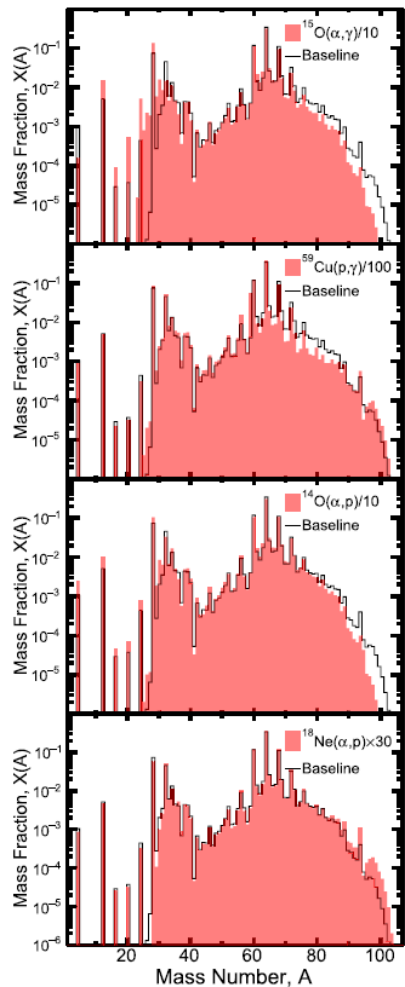


Energy levels of ^{22}Ne					
ETCM calculation			Experimental data		
J^π	E_x (MeV)	θ_α^2 (%)	J^π	E_x (MeV)	θ_α^2 (%)
1 ⁻	12.58	13	1 ⁻	12.58	10
1 ⁻	13.53	8	1 ⁻	12.84	20
3 ⁻	12.92	13	3 ⁻	13.19	19
3 ⁻	13.69	11	3 ⁻	13.41	11

As can be seen in Fig. 9 there are many anomalies in the ^{22}Mg spectrum at lower energies. The corresponding resonances were not observed in the mirror $\alpha + ^{18}\text{O}$ scattering due to the very small energies of the α particles. Generally speaking, a proper study of $\alpha + ^{18}\text{Ne}$ can bring information about the states in ^{22}Ne which are very close to the α -particle threshold, and maybe even below it.

TABLE II. Tentative spin assignment for ^{22}Mg levels.

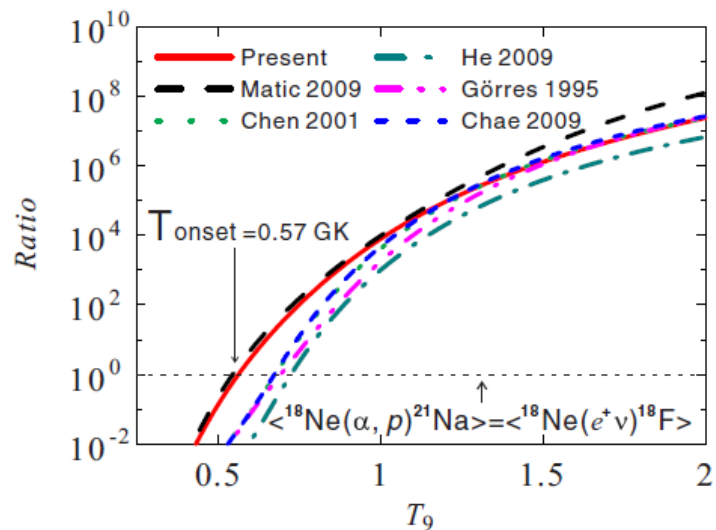
Level	Spin	Energy (MeV)
1	2	2.87
2	2	3.055
3	0	3.18
4	1	3.32
5	2	3.656
6	1	3.70
7	0	3.76
8	1	4.02
9	0	4.021
10	2	4.085
11	1	4.22



11410	8	A	
11499	17	K	[2+]
11594	12	KL	
11748	17	KL	[0+]
11914	13	KL	
12003	20	?	L
12185	17	KL	[3-]
12474	26	K	[2+]
12665	17	K	[3-]
13014	37	A	K
14012	3	A	G

TABLE I. Resonant parameters used in the present R -matrix analysis.

E_x (^{22}Mg)	J^π	s	ℓ	Γ_p (keV)
6.333	1^+	1	0	16
6.591	1^-	2	1	36
6.615	2^+	2	0	10
6.796	2^-	1	1	62
6.885	1^-	2	3	2
7.270	1^-	2	1	82
7.339	2^+	2	2	18
7.369	3^-	2	3	7
7.585	2^+	2	0	16
7.654	1^-	2	1	114
7.802	2^-	1	1	19
7.920	2^+	2	0	3
8.005	3^-	2	3	1
8.190	2^+	2	2	5
8.353	1^+	1	2	97
8.527	3^-	2	1	3
8.578	4^+	2	2	5
8.677	2^+	2	2	7
8.727	2^+	2	0	12
8.827	1^-	2	1	57
8.922	2^+	2	2	4
9.050	1^-	2	1	105
9.158	4^+	2	2	2



As discussed in the Introduction, the $^{18}\text{Ne}(\alpha, p)^{21}\text{Na}$ cross section was studied before by Bradfield-Smith *et al.* [9] and Groombridge *et al.* [10]. There, the experimental results were summarized as a table of resonance parameters and widths. Figure 14 displays the cross section derived from the resonance parameters of Ref. [10], in comparison to our result. Our experiment shows a much lower cross section, by close to an order of magnitude.

TABLE I. Resonant properties of excited states in ^{22}Mg deduced from the present work. The excitation energies from the previous work are listed for comparison. The uncertainties of energy, in units of keV, are included in parentheses. The observed proton partial widths are deduced from the R -matrix analysis with those spin-parity assignments as shown in Fig. 1.

E_x^{present}	E_x [7]	E_x [8]	E_x [9]	E_x [11]	Parity ^a	J^π (R matrix) ^b	$J^\pi; \ell$ (adopted)	Γ_p (keV)
6.61(15) ^c	6.606(9)	6.606(11)	6.616(4)		$\pi = \text{N}$ [4]	$(2^+, 1^+)$	$2^+; 0$	23(7)
6.81(15) ^d	6.766(12)	6.767(20)	6.771(5)	6.760(90)		$(1^+, 2^+)$	$(1^+, 2^+); 0$	64(20)
6.93(15)		6.889(10)	6.878(9)		$\pi = \text{N}$	$(2^+, 1^+, 3^-, 2^-)$	$(2^+, 3^-); 0(1)$	27(7)
7.06(16)						$(1^+, 3^-, 2^-)$	$(1^+, 3^-, 2^-); 0(1)$	49(20)
7.27(16)						$(2^+, 1^+)$	$(2^+, 1^+); 0$	17(7)
7.42(17)		7.402(13)	7.373(9)			$(1, 2^+)$	$(1, 2^+); 0(1)$	10(7)
7.59(17)	7.614(9)		7.606(11)			$(1^+, 2^+)$	$(1^+, 2^+); 0$	23(7)
7.82(18)		7.784(18)	7.757(11)	7.840(90)	$\pi = \text{uN}$	$(1^- - 3^-)$	$(2^-); 1$	27 ^g
7.98(19)	7.938(9)	7.964(16)	7.986(16)	7.890(100)	$\pi = \text{N}$	$(1^+, 2^+)$	$(2^+); 0$	20 ^g
8.18(19)	8.197(10)	8.203(23)	8.229(20)			$(1^+ - 3^+)$	$(1^+ - 3^+); 2$	33 ^g
8.31(20)				8.290(40)		$(1^+ - 3^+)$	$(1^+ - 3^+); 2$	49 ^g
8.51(20) ^e	8.512(10)	8.547(18)		8.550(90)	$\pi = \text{N}$	$(1^- - 3^-)$	$(3^-); 1$	60(20)
8.62(21) ^f	(8.644(18))	8.613(20)	8.598(20)			(2^+)	$(2^+); 2$	33(10)

^aN, uN denote level of natural and unnatural parity, respectively.

^bPresent results deduced from the R -matrix analysis.

^c $J^\pi = 2^+$ determined for the 6.616-MeV state [16].

^d $J^\pi = (1^-, 2^-)$ determined for the 6.796-MeV state [16].

^e $J^\pi = 2^+$ assumed in Chen *et al.* [8].

^f $J^\pi = 3^-$ assumed in Chen *et al.* [8].

^gThe proton widths of these states are only roughly estimated from the R -matrix fits to the data.

Present work			
E_x (MeV)	Γ_α (keV)	J^π	θ_a^2 (%)
11.493	7	1^-	4.78
11.705	3	3^-	12.30
11.869	6	1^-	2.40
12.352	19	1^-	3.72
		(4^+)	
12.744	11	3^-	6.80
12.974	8	3^-	3.65
13.456	4	3^-	1.06
		$(0^+, 1^-)$	
13.644	177	0^+	11.0
		$(1^-, 4^+, 5^-)$	
14.381	16	4^+	5.01
		$(2^+, 5^-)$	
15.199	15	4^+	2.49
		$(2^+, 3^-)$	
15.477	4	5^-	1.59
		$(0^+ \text{ to } 7^-)$	

TABLE II. Tentative spin assignment for ^{22}Mg levels.

Level	Spin	Energy (MeV)
1	2	2.87
2	2	3.055
3	0	3.18
4	1	3.32
5	2	3.656
6	1	3.70
7	0	3.76
8	1	4.02
9	0	4.021
10	2	4.085
11	1	4.22

TABLE I. Summary of resonance parameters ($R=5.0$ fm).

N	$E_{\text{c.m.}}$ (MeV)	E_x (MeV)	J^π	$\Gamma_{\text{c.m.}}$ (keV)	$\Gamma_\alpha / \Gamma_{\text{tot}}$ %	γ_α^2 (keV)	$\gamma_\alpha^2 / \gamma_\pi^2$ %
1	2.91	12.58	1^-	97	36	79	10
2	3.17	12.84	1^-	145	72	150	20
3	3.52	13.19	3^-	67	40	144	19
4	3.74	13.41	3^-	56	40	82	11
5	9.61	19.28	(7^-)	88	25	64	8
6	9.89	19.56	(7^-)	75	23	41	5
7	11.18	20.85	9^-	110	14.5	393	51
8	12.17	21.84	9^-	170	22.	441	57

TABLE VII. The spin values and resonance strengths of the levels at center-of-mass energies E_{res} (c.m.) used in the calculations of the rates for the $^{18}\text{Ne}(\alpha, p)^{21}\text{Na}$ reaction.

E_x (MeV)	E_{res} (c.m.) (MeV)	$J^{\pi a}$	S_{α}	Γ_{α} (eV)	$\omega\gamma$ (eV)
8.1812(16)	0.039	[2 ⁺]	2.8×10^{-1}	1.7×10^{-65}	8.53×10^{-65}
8.385(7)	0.243	[2 ⁺]	3.2×10^{-1}	2.7×10^{-18}	1.33×10^{-17}
8.5193(20)	0.377	[3 ⁻]	4.0×10^{-3}	7.0×10^{-15}	4.87×10^{-14}
8.574(6)	0.432	[4 ⁺]	6.0×10^{-2}	3.6×10^{-13}	3.26×10^{-12}
8.6572(17)	0.515	[0 ⁺]	1.1×10^{-1b}	5.0×10^{-8}	4.97×10^{-8}
8.743(14)	0.601	[4 ⁺]	2.2×10^{-2}	5.7×10^{-10}	5.15×10^{-9}
8.7832(22)	0.642	[1 ⁻]	1.1×10^{-1b}	4.0×10^{-6}	1.21×10^{-5}
8.9318(27)	0.790	[2 ⁺]	1.1×10^{-1b}	8.3×10^{-5}	4.13×10^{-4}
9.080(7)	0.938	[1 ⁻]	1.1×10^{-1b}	7.7×10^{-3}	2.31×10^{-2}
9.157(4)	1.015	[4 ⁺]	7.8×10^{-2}	9.7×10^{-5}	8.70×10^{-4}
9.318(12)	1.176	[2 ⁺]	1.1×10^{-1b}	9.9×10^{-2}	4.97×10^{-1}
9.482(11)	1.342	[3 ⁻]	1.5×10^{-2}	1.8×10^{-2}	1.25×10^{-1}
9.542(9)	1.401	[2 ⁺]	2.8×10^{-2}	3.6×10^{-1}	1.78
9.709(19)	1.565	[0 ⁺]	1.5×10^{-1}	5.2×10^1	5.18×10^1
9.7516(27)	1.610	[2 ⁺]	1.9×10^{-2}	1.6	8.22
9.860(5)	1.718	[0 ⁺]	1.9×10^{-2}	2.1×10^1	2.07×10^1
10.085(13)	1.944	[2 ⁺]	5.0×10^{-2}	4.5×10^1	2.25×10^2
10.2715(17)	2.130	2 ⁺	$_{-c}$	$_{-c}$	1.03×10^{4c}
10.429(13)	2.287	[4 ⁺]	$_{-c}$	$_{-c}$	7.30×10^{3c}
10.651(13)	2.513	[3 ⁻]	$_{-c}$	$_{-c}$	1.82×10^{4c}
10.768(13)	2.626	[2 ⁺]	1.1×10^{-1b}	2.3×10^3	1.16×10^4
10.873(14)	2.734	[0 ⁺]	$_{-c}$	$_{-c}$	4.52×10^{4c}
11.001(11)	2.859	[4 ⁺]	$_{-c}$	$_{-c}$	8.10×10^{3c}
11.315(16)	3.173	[4 ⁺]	3.0×10^{-2b}	2.0×10^2	1.83×10^3
11.499(17)	3.357	[2 ⁺]	1.1×10^{-1b}	1.7×10^4	8.64×10^4
11.595(12)	3.455	[1 ⁻]	5.4×10^{-2}	2.0×10^4	6.11×10^4
11.747(17)	3.607	[0 ⁺]	1.1×10^{-1b}	7.1×10^4	7.13×10^4
11.914(13)	3.780	[0 ⁺]	1.1×10^{-1b}	8.8×10^4	8.82×10^4
12.003(20)	3.861	[1 ⁻]	2.1×10^{-1}	1.4×10^5	4.31×10^5
12.185(17)	4.050	[3 ⁻]	1.8×10^{-1}	3.7×10^4	2.60×10^5
12.474(26)	4.332	[2 ⁺]	1.1×10^{-1b}	7.8×10^4	3.89×10^5
12.665(17)	4.523	[3 ⁻]	1.2×10^{-1}	4.9×10^4	3.45×10^5
(13.010(50))	4.865	[0 ⁺]	1.1×10^{-1b}	2.2×10^5	2.16×10^5

^aSpin for the mirror assignments given in Figs. 9 and 10.

^bConstant S_{α} values as explained in the text.

^cResonance strengths are measured in Ref. [22].

present (p,t) (MeV)	adopted energy (MeV)		
(13.01(5))	13.01 [0+]	13.384 (4+)	13.131 4+ T
		13.274 (0+)	13.027 0+ T
		13.078 (4+)	12.983 4+ T
		12.910 (1+)	12.768 1+ T
		12.862 (3-)	
		12.820	(1-)#
		12.800	(2+)
		12.760	(3-)
		12.643	(2+)
		12.570	(1-)#
		12.450(0+,1-)	
		12.390 3-	(2+)
		12.280	(1-)#
		12.218	(0+)
		12.071	(0+)
		12.000 (4+)	12.037 4+ T
		11.896	(1-)
		11.772 3-	(1-)
		11.708 (1-)	(2+)
		11.656 (1+)	11.736 1+ T
		11.577 (4+)	11.696 4+ T
		11.533 (6+)	11.655 6+ T
		11.465 3-	
		11.433 (2+)	11.477 2+ T
		11.271 (4+)	11.453 4+ T
		11.194 (0+)	11.407 0+ T
		11.130 (6,7)	
		11.064 2+	
		11.001 [4+]	
		11.032 (8+)	
		10.921 1-	
		10.857 3-	
		10.749 (4+)	10.756 4+ T
		10.706 (0+)	10.639 0+ T
		10.696 (3+)	10.579 3+ T
		10.616 (7+)	10.549 7+ T
		10.551 2+	
		10.493 2+	
		10.469 3-	
		10.423 (3+)	10.325 3+ T
		10.384 (6+)	10.270 6+ T
		10.297 (0,1,2)	
		10.282 (0,1,2)	

²²Mg

²²Ne

